Materials Science Forum 649 (2010) pp 349-354
© (2010) Trans Tech Publications, Switzerland
doi:10.4028/www.scientific.net/MSF.649.349

Columnar to Equiaxed Transition During Ingot Casting Using Ternary Alloy Composition

L. Könözsy[1,a], A. Ishmurzin[2,a], M. Grasser[2,b], M. Wu[2,c], A. Ludwig[2,d], R. Tanzer[3,a] and W. Schützenhöfer[3,b]

[1] Christian Doppler Laboratory for Multiphase Modeling of Metallurgical Processes, University of Leoben, A-8700 Franz-Josef Str. 18, Leoben, Austria

[2] Department of Metallurgy, Chair for Simulation and Modeling of Metallurgical Processes, University of Leoben, A-8700 Franz-Josef Str. 18, Leoben, Austria

[3] Böhler Edelstahl GmbH & Co KG, Kapfenberg, Austria

[1,a]laszlo.koenoezsy@mu-leoben.at, [2,a]anton.ishmurzin@mu-leoben.at, [2,b]monika.grasser@mu-leoben.at, [2,c]menghuai.wu@mu-leoben.at, [2,d]andreas.ludwig@mu-leoben.at, [3,a]robert.tanzer@bohler-edelstahl.at, [3,b]wolfgang.schuetzenhoefer@bohler-edelstahl.at

Keywords: multiphase flows, numerical methods, solidification, melting, columnar to equiaxed transition, ternary alloy compostion, macrosegregation

Abstract. The present paper deals with the formation of macrosegregation in a benchmark ingot using (Fe-C-Cr) ternary alloy composition. The numerical investigation of complex multiphase phenomena is a difficult study, because the thermophysical properties depend strongly on the temperature, concentration, pressure and chemical composition as well. For the numerical modeling of solidification and melting processes different phases (e.g. liquid, equiaxed crystals and columnar dendrite trunks) have been considered. The mass, momentum, energy conservation and species conservation equations for each phase have been solved. The Eulerian-Eulerian model equations have been implemented in the commercial Finite Volume Method based FLUENT-ANSYS v6.3 CFD software using User-Defined Functions (UDF). The mass transfer has been modelled by diffusion controlled crystal growth by applying an advanced tip tracking algorithm for columnar solidification. The modeling of the grain density transport has been improved. The derivatives of the mass fraction quantities for each component appear in the nucleation rate term. It means that we obtain a new term of the right hand side of the grain density transport equation for using ternary alloy composition. This paper focuses on both the process and simulation parameters and their influence on the macrosegregation formation. The results show that the macrosegregation pattern does not change significantly above a well-chosen number of grid cells, and the computational time could be decreased, when the time step size has been increased.

Introduction

The multicomponent solidification and melting processes plays an important role in the field of multiphase modeling [1-9]. Gu [1] and Beckermann [1-3] used a model to study the multicomponent macrosegregation with numerical solution of fully coupled mass, momentum, energy and species conservation equations for an industrial steel ingot. The model was applied to investigate the macrosegregation and the flow field considering also thermal and solutal convections. The present work is a recent development and application of the volume averaged multiphase and multicomponent (Fe-C-Cr) model by Ludwig et al [4] and Wu et al [5-6]. The model was validated by Tanzer et al [7] in the case of a cast benchmark ingot at the Böhler Edelstahl GmbH & Co KG (BEG) in Kapfenberg, Austria. The numerical results have been explained considering the process parameters such as the thermal and solutal convection and the nucleation parameters based on a parameter study by Könözsy et al [8]. The multicomponent modeling is a relevant outcome of the CDL & BEG cooperation coupling solidification kinetics with thermodynamics. This method has been developed and implemented by Ishmurzin et al [9].

Brief description of the multiphase Eulerian-Eulerian model

A volume averaged Eulerian-Eulerian multiphase solidification and melting model was developed for multicomponent alloy system. Three phases are considered, namely liquid phase *l*, columnar dendrite trunks *c* and equiaxed grains *e*. The morphology of the equiaxed grains was approximated by ideal spheres. The growth velocity of equiaxed grain were analytically derived [4-6] as

$$v_{R_e} = \frac{2D_j}{d_e} \cdot \frac{\tilde{c}_l^j - c_l^j}{\tilde{c}_l^j - \tilde{c}_e^j}, \tag{1}$$

where D_j is the diffusion coefficient of the *j*-th species in the liquid, d_e is the diameter of equiaxed grains, c_l^j is the liquid mass fraction of the *j*-th species, $\tilde{c}_l^j$ and $\tilde{c}_e^j$ are the equilibrium mass fractions at the liquid/solid interface. The momentum equation for the columnar phase was not solved, because the dendrite tip was tracked by an explicit type algorithm using the LGK [10] model. The distance between two cylinder centers represents the primary dendrite arm spacing λ_1. The growth velocity of columnar dendrite trunks was analytically derived [4-6] as

$$v_{R_c} = \frac{2D_j}{d_c} \cdot \frac{\tilde{c}_l^j - c_l^j}{\tilde{c}_l^j - \tilde{c}_c^j} \cdot \ln^{-1}\left(\frac{d_{\max}}{d_c}\right), \tag{2}$$

where $d_{\max}$ is the maximal diameter available for cylindrical growth, d_c is the actual diameter of columnar dendrite trunks, $\tilde{c}_c^j$ is the equilibrium mass fraction of the columnar solid at the liquid/solid interface. Considering a hexagonal dendrite arrangement with dendrite arm spacing λ_1, the maximal diameter can be chosen as $d_{\max} = 1.05 \cdot \lambda_1$. The mass transfer rate from the liquid to the equiaxed phase was defined as

$$M_{le} = v_{R_e} \cdot \left(n \cdot \pi \cdot d_e^2\right) \cdot \rho_e \cdot f_{imp}, \tag{3}$$

where ρ_e is the density of the equiaxed phase, f_{imp} is the impingement factor [11]. The mass transfer rate from the liquid to columnar phase was defined as

$$M_{lc} = v_{R_c} \cdot \left(\frac{2\sqrt{3} \cdot \pi \cdot d_c}{3\lambda_1^2}\right) \cdot \rho_c \cdot f_{imp}, \tag{4}$$

where ρ_c is the density of the columnar phase, V_{tip} is the tip velocity, and R_{tip} is the tip radius. The impingement factors are different for the spherical and cylindrical growth. An Avrami-type factor was used ($f_{imp} = f_l$) for equiaxed solidification. The impingement factor for columnar solidification was assumed as

$$f_{imp} = \begin{cases} 1, & 0 < d_c \le \lambda_1, \\ 1 - \dfrac{d_c - \lambda_1}{d_{\max} - \lambda_1}, & \lambda_1 < d_c \le d_{\max}. \end{cases} \tag{5}$$

The volume averaged and equilibrium mass fractions $c_l^j, \tilde{c}_l^j, \tilde{c}_e^j, \tilde{c}_c^j$ for the estimation of growth velocities are computed by solving a non-linear algebraic system of equations. The process-related quantity c_l^j and the thermo-dynamic-related quantities $\tilde{c}_l^j, \tilde{c}_e^j, \tilde{c}_c^j$ are coupled with corresponding

Fe-C-Cr phase diagram information [9]. After computing the mass transfer rates, the multiphase Eulerian-Eulerian approach is applied to consider the mass, momentum, enthalpy and species conservations. The mass transfer rate from the columnar to the equiaxed phase is neglected. The grain sedimentation is taken into account by solving the momentum equation for the equiaxed phase. The size of the grains is controlled by a packing limit in order to obtain realistic mass transfer values during the grain-to-grain interaction in the control volume. Thermal and solutal buoyancy are modeled by using the Boussinesq approach. In order to study the macrosegregation quantitatively, the mixture concentration is defined as

$$c_{mix}^{j}=\frac{c_l^j\cdot\rho_l^j\cdot f_l^j+c_e^j\cdot\rho_e^j\cdot f_e^j+c_c^j\cdot\rho_c^j\cdot f_c^j}{\rho_l^j\cdot f_l^j+\rho_e^j\cdot f_e^j+\rho_c^j\cdot f_c^j}. \tag{6}$$

The conservation of the number density n of the equiaxed grains was considered as

$$\frac{\partial n}{\partial t}+\nabla\cdot(\mathbf{u}_e n)=\frac{d(\Delta T)}{dt}\cdot\frac{n_{\max}}{\sqrt{2\pi}\cdot\Delta T_\sigma}\cdot e^{-\frac{1}{2}\left(\frac{\Delta T-\Delta T_N}{\Delta T_\sigma}\right)^2}, \tag{7}$$

where $n_{\max}$ is the maximal available nucleation sites, $\Delta T=T_L\left(c_l^\alpha,c_l^\beta\right)-T_l$ is the constitutional undercooling, ΔT_N is the undercooling for maximum grain production rate, and ΔT_σ is the Gaussian distribution width of the nucleation law. This approach was developed by Oldfield suggesting a continuous distribution of nucleation sites [12]. For modeling ternary alloy composition, the derivatives of the liquidus temperature and c_l^α, c_l^β liquid mass fractions appear in the right hand side of the grain density transport equation

$$\frac{\partial n}{\partial t}+\frac{\partial(u_e n)}{\partial x}+\frac{\partial(v_e n)}{\partial y}+\frac{\partial(w_e n)}{\partial z}=\left[\frac{\partial(\Delta T)}{\partial t}+u_l\left(\frac{\partial T_L}{\partial c_l^\alpha}\frac{\partial c_l^\alpha}{\partial x}+\frac{\partial T_L}{\partial c_l^\beta}\frac{\partial c_l^\beta}{\partial x}-\frac{\partial T_l}{\partial x}\right)+\right.$$
$$\left.+v_l\left(\frac{\partial T_L}{\partial c_l^\alpha}\frac{\partial c_l^\alpha}{\partial y}+\frac{\partial T_L}{\partial c_l^\beta}\frac{\partial c_l^\beta}{\partial y}-\frac{\partial T_l}{\partial y}\right)+w_l\left(\frac{\partial T_L}{\partial c_l^\alpha}\frac{\partial c_l^\alpha}{\partial z}+\frac{\partial T_L}{\partial c_l^\beta}\frac{\partial c_l^\beta}{\partial z}-\frac{\partial T_l}{\partial z}\right)\right]\cdot\frac{n_{\max}}{\sqrt{2\pi}\cdot\Delta T_\sigma}\cdot e^{-\frac{1}{2}\left(\frac{\Delta T-\Delta T_N}{\Delta T_\sigma}\right)}. \tag{8}$$

Since $d(\Delta T)/dt$ is the substantial derivative of the undercooling, therefore an unsteady and a convective term will appear according to the time, the mass fractions and the coordinates. For modeling the nucleation process accurately, this term has to be handled and implemented numerically related to the phase diagram information. The Gaussian distribution was chosen for modeling the distribution width of the nucleation law, because this approach showed good agreement with experimental data in a previously tested cast ingot by the industrial partner [7]. Further details about the multiphase volume averaging model can be found in the literature [4-9].

Results and discussion

The solidification of a ternary steel ingot (X34Cr15) with a relatively small size (diameter: 66 mm, height: 170 mm) was set up for CFD simulations (see Table 1). The number of grid cells has been increased from 180 to 4300 in half of the symmetrical domain. The aim of the CFD code development process was to increase the numerical stability and accuracy of the solution to have a possibility to use bigger time step sizes confidently than earlier, which is a good opportunity to decrease the computational time. The computational time was 3 days with 0.001 seconds time step size with converged solution, and it was only approximately 3 hours employed time step of 0.1 seconds. All properties and parameters used for the simulation are listed in Table 1.

Table 1. *Material properties, process parameters and initial conditions for CFD simulation*

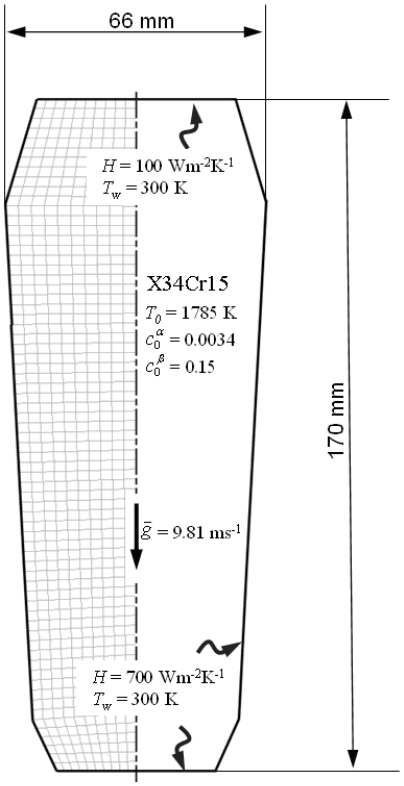

Thermophysical properties:

$c_{p(l)} = c_{p(s)} = 804$ (Jkg^{-1}K^{-1})

$D_l = 2 \cdot 10^{-8}$ (m^{2}s^{-1})

$D_e = D_c = 5.6 \cdot 10^{-10}$ (m^{2}s^{-1})

$\Delta h_f = h_l^{ref} - h_e^{ref} = 256476$ (Jkg^{-1})

$k_l = k_e = k_c = 31.3$ (Wm^{-1}K^{-1})

$\beta_T = 0.0002$ (K^{-1})

$\beta_c^C = 0.011$ (wt.%$^{-1}$)

$\beta_c^{Cr} = 0$ (wt.%$^{-1}$)

$\rho_l = \rho_e = \rho_c = 7270$ (kgm^{-3})

$\Delta\rho = \rho_l - \rho_{e/c} = 269$ (kgm^{-3})

Thermodynamics properties:

$\Gamma = 2.9 \cdot 10^{-7}$ (mK)

Process parameters:

$n_{\max} = 5 \cdot 10^9$ (m^{-3})

$\Delta T_N = 5$ (K)

$\Delta T_\sigma = 2$ (K)

The solidification starts, when the temperature is close to the mould below liquidus. The equiaxed grains start to sink, and induce melt convection. The melt is dragged by the sinking grains downwards along the wall, which in turn induces a rising melt flow in the middle of the casting driven by thermal and solute buoyancy. From the flow pattern of Fig. 1 and Fig 2, it can be seen that the combined effect of thermal buoyancy and equixed grain sedimentation induced flow dominates the overall convection pattern.

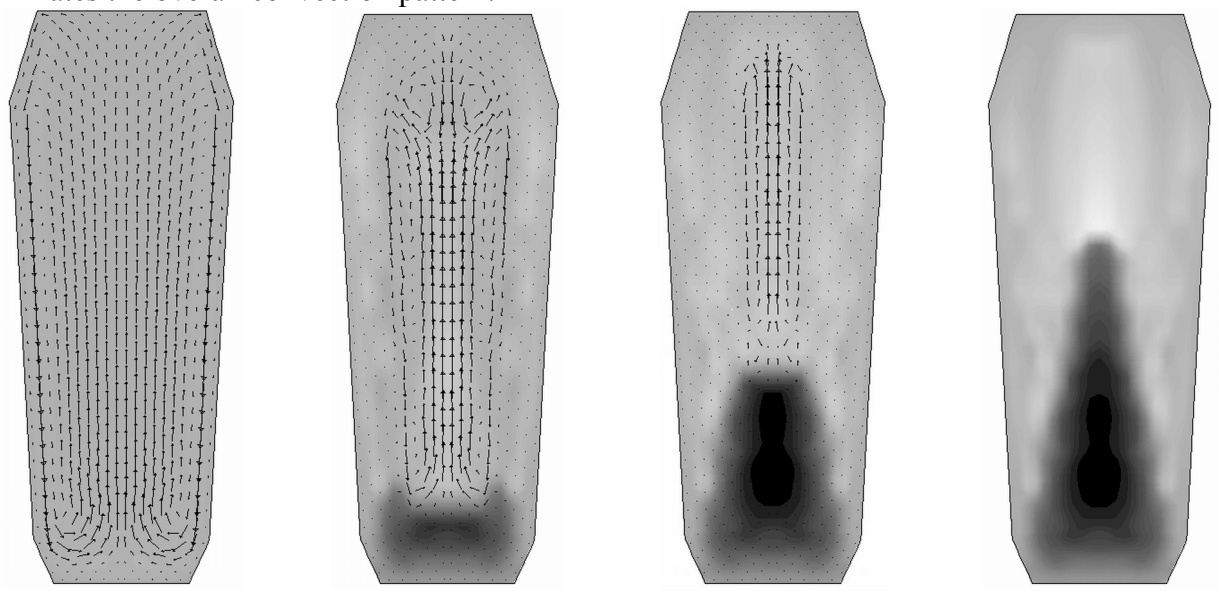

2s 20s 50s 100s

Figure 1. *Predicted macrosegregation patterns overlaid with liquid velocity vectors for the Carbon component; the middle value of the grey scale is 0.34wt.% initial concentration.*

The grains sink down and settle at the bottom region. Furthermore, the grains continue to nucleate, sink and grow. They settle and pile up in the lower region of the ingot. As we do not consider any nucleation barrier for solidification at the mould wall, columnar dendrites start to grow from the mould wall towards the bulk melt. Whether the melt rises or sinks depends strongly on the value of the thermal and solutal expansion coefficients. Thermal buoyancy leads to an overall downwards motion near the mould wall and an upwards motion in the centre of the ingot. The smaller equiaxed crystals follow this general flow pattern. The CFD simulations predict a chance of having smaller crystals flowing first downwards and then upwards. These upwards flowing grains face high temperatures at the centre of the ingots and tend to melt again. The grain sedimentation results in the well-known cone-shaped equiaxed region at the ingot bottom. As consequence a cone-shaped region of negative macrosegregation forms (see Fig. 1-2). Due to the fact that the nucleation parameters (see Table 1) are not known specifically for the ternary alloy of interest, we have adjusted them according to experiments provided by the industrial partner [7-8].

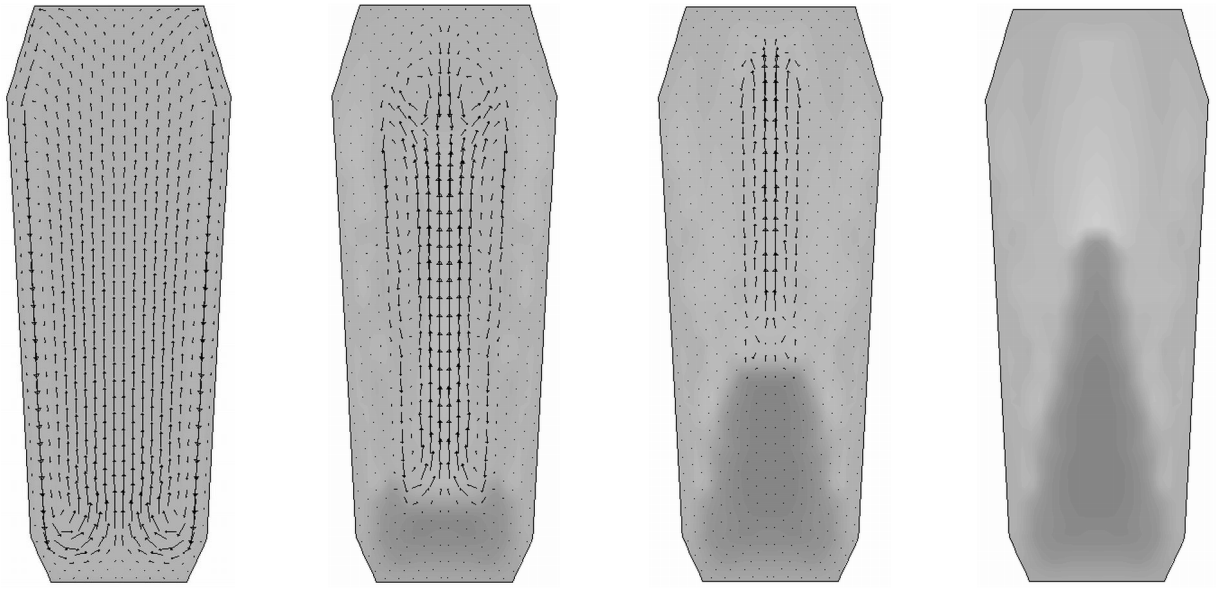

Figure 2. *Predicted macrosegregation patterns overlaid with liquid velocity vectors for the Chromium component; the middle value of the grey scale is 15wt.% initial concentration.*

The solidification of the whole casting is completed at $t = 100$ s. The positive segregation zone which forms at the top part of the ingot is mainly due to melt convection as well. The solute rich melt rises as the equiaxed grains sink. The rising melt transports solute rich melt from the bottom region towards the top in the casting center. As the melt hits the casting top, it diverges into side streams, resulting in a positive segregation in the upper region of the ingot as shown in Fig. 1-2. The positive centre macrosegregation occur at the end of the solidification, therefore enriched melt to solidify. This positive segregation at the top is also explained by convection of segregated melt from ingot center which coincides qualitatively with the experimental results of Nakagawa et al [13]. A columnar-to-equiaxed transition (CET) occurs at the end of solidification when the growing columnar dendrite tips are blocked by equiaxed grains. Two types of 'blocking' mechanisms exist. One of them is due to the 'mechanical blocking' when the local volume fraction of equiaxed grain envelopes exceeds a certain limit, the other one is due to the 'soft-blocking' phenomena when the local constitutional undercooling disappears [4-6]. The predicted macrosegregation pattern of Carbon and Chromium have different magnitudes according to Fig. 1-2, although the patterns for the two elements look similar. For Carbon deviations from the initial composition by about ±42% and Chromium by about ±8% are predicted. The differences are caused by the fact that the back

diffusion was not taken into account in the model. Finally, it has to be mentioned that channel segregations, which are frequently reported in steel ingots, are not predicted with the recent model.

Summary

A multiphase model and a Finite Volume Method (FVM) based FLUENT-ANSYS v6.3 CFD code were developed to simulate a benchmark ingot casting with a ternary X34Cr15 alloy composition. The aim of the code development was to increase the numerical stability and accuracy of the numerical solution of the proposed Eulerian-Eulerian multiphase volume averaged model equations. It was a good opportunity to perform parameter and grid study for macrosegregation in ingot casting. The number of grid cells has been increased from 180 to 4300 to define an optimal grid size, to prove the reliability of model implementation. The results show that the macrosegregation pattern does not change significantly above a well-chosen number of grid cells, at least from 2780 cells in our case. The grain density transport equation for ternary alloy composition has been improved. The derivatives of the mass fraction quantities for each component appear in the nucleation rate term. The sedimentation of the equiaxed grains, the movement of the columnar dendrite tip and the formation of macrosegregations were considered in the model. The results support the well-known explanation of ingot casting process by Campbell [14].

Aknowledgements

This work is financially supported by the Austrian Christian-Doppler Research Society, and Böhler Edelstahl GmbH & Co KG for which the authors kindly acknowledge. The authors wish to express their appreciation to FLUENT-ANSYS Inc. for their technical assistance.

References

[1] J. P. Gu and C. Beckermann: Metall. Mater. Trans., Vol. 30A (1999), pp. 1357-1366

[2] C. Beckermann: Presented at the Flemings Symposium, Boston, MA (2000)

[3] C. Beckermann: Material Reviews, Vol. 47/5 (2002), pp. 243-261.

[4] A. Ludwig and M. Wu: Mat. Sci. Eng., Vol. A413-414 (2005), pp. 109-114

[5] M. Wu and A. Ludwig: Metall. Mater. Trans., Vol. 37A (2006), pp. 1613-1631

[6] M. Wu and A. Ludwig: Metall. Mater. Trans., Vol. 38A (2007), pp. 1465-1475

[7] R. Tanzer, W. Schützenhöfer, G. Reiter, H.-P. Fauland, L. Könözsy, A. Ishmurzin, M. Wu and A. Ludwig: *Proceedings of the 2007 International Symposium on Liquid Metal Processing and Casting* (LMPC'2007), Nancy, France (2007), pp. 121-126

[8] L. Könözsy, F. Mayer, A. Ishmurzin, A. Kharicha, M. Wu., A. Ludwig, R. Tanzer and W. Schützenhöfer: Proc. ASMET–STEELSIM, Seggau, Austria (2007), pp. 126-132

[9] A. Ishmurzin, M. Gruber-Pretzler, F. Mayer, M. Wu and A. Ludwig: Int. J. Mat. Res., Vol. 99(6) (2008), pp. 618-625

[10] J. Lipton, M.E. Glicksman and W. Kurz: Mater. Sci. Eng., Vol. 65 (1984), pp. 57-63

[11] F. Mayer, M. Gruber-Pretzler, L. Könözsy, M. Wu and A. Ludwig: Proc. ASMET–STEELSIM, Seggau, Austria (2007), pp. 265-270

[12] W. Oldfield: Trans. ASM, Vol. 59 (1966), pp. 945-961

[13] Y. Nakagawa and A. Momose: Tetsu-to-Hagane, Vol. 53 (1967), pp. 1477-1508

[14] J. Campbell: Castings, Butterworth Heinemann Ltd., Oxford (1991), pp. 151-158